ORIENTAL JOURNAL OF CHEMISTRY
An International Open Access, Peer Reviewed Research Journal
www.orientjchem.org
ISSN: 0970-020 X
CODEN: OJCHEG
2025, Vol. 41, No.(2):
Pg. 609-615

Screw Pine Cellulose Reinforced Polylactic acid Nanocomposites: Thermal, Structural and Antibacterial Insights

PRIYA SA[1]* and NEVADITHA NT[2]

[1*,2]Department of Chemistry & Research, Nesamony Memorial Christian College, Marthandam-629165, Tamil Nadu, India.
Affiliated with Manonmaniam Sundaranar University, Tirunelveli-627012, Tamil Nadu India.
*Corresponding author E-mail: sathyarajsathya1961@gmail.com

http://dx.doi.org/10.13005/ojc/410230

(Received: November 22, 2024; Accepted: March 05, 2025)

ABSTRACT

Polylactic acid (PLA) is a compostable and Eco-friendly polymer ideal for environmentally conscious applications. Enhancements with crosslinkers and fiber reinforcement improve its properties, making PLA suitable for innovative packaging, biomedical, and sustainable materials. This study aims to enhance PLA's performance by incorporating cellulose nanofibers (CNFs) from screw pine leaves using chemico-mechanical method. The nanocomposites were fabricated by blending 1wt% and 2wt% CNFs into PLA using the solution casting approach. FTIR analysis of the PLA nanocomposites show a peak at 1254 cm^{-1}, confirming C–O stretching vibrations of CNFs in the polymer matrix, while a stronger broad peak at 3418 cm^{-1} indicates enhanced hydrogen bonding and improved compatibility. Thermal analysis shows that adding 2wt% CNFs to PLA increases the decomposition temperature by 6°C, indicating enhanced thermal stability. SEM confirms even CNF distribution in the PLA matrix, suggesting effective dispersibility and strong interfacial interactions. Additionally, increasing the CNF content significantly improved the antibacterial activity of the PLA nanocomposite films against *E. coli* and *S. aureus*. These findings suggest that PLA nanocomposites are promising for sustainable applications, particularly in packaging and healthcare, where biodegradability and antibacterial properties are essential.

Keywords: Polylactic acid, Screw pine fibers, Nanocomposites, Thermal, Antibacterial properties.

INTRODUCTION

Polylactic acid (PLA) is a bio-based thermoplastic sourced from carbohydrate sources, such as corn and wheat. It is regarded as a promising bio-based alternative to petroleum-derived polymers[1]. Due to its impressive stiffness and strength, PLA has emerged as a valuable material in various fields, including packaging, the automotive industry, and biomedical applications[2,3]. Although PLA can be utilized in a diverse array of applications, including those involving synthetic polyethylene and polypropylene polymers, its fundamental brittleness, low crystallization degree, and relatively insufficient thermal stability constrain its potential for widespread application[4]. The full integration of PLA as a sustainable material requires the addition of suitable fillers and an enhancement in its properties[5].

The utilization of cellulose nanofibers (CNFs), obtained from renewable biomass, has gained considerable interest as a potential replacement for micro-sized reinforcements in composite material applications[6]. It is often employed as a reinforcing filler in various polymeric substances, including polyvinyl alcohol (PVA), natural rubber, and polylactic acid (PLA)[7]. Cellulose from fibers like cotton, flax, hemp, jute, and sisal is used to reinforce polymers because of its strength, rigidity, and lightweight properties[8]. Moreover, the inclusion of nanocellulose not only strengthens the reinforcing effect capabilities and simultaneously enhances the material's biodegradability[9]. Pandanus odoratissimus, commonly referred to as screw pine, is member of the Pandanaceae family and is originally found in South Asia and India. This species is distinguished by its long, spiky green leaves, which are composed of 52% cellulose. The mechanical properties of the leaves are regarded as highly advantageous when compared to those of pineapple leaves, which facilitates their use in the creation of a range of traditional products, such as mats, baskets, hats, fans, pillows, and various other woven artifacts[10]. The therapeutic properties of essential oil derived from the fragrant flowers of the screw pine have been found to be beneficial in alleviating headaches, earaches, and serving as a liniment for rheumatic discomfort[11].

The isolation of nanocellulose can be achieved using several approaches, including acid hydrolysis, steam explosion, and mechanical methods[12]. The hydrophilic characteristics of cellulose result in its inadequate dispersion within PLA polymer that exhibits hydrophobic properties. Effective dispersion of nanofillers within the polymer matrix is crucial for achieving performance improvements over the unaltered polymer[13]. Accordingly, this study focused on the synthesis of CNFs derived from screw pine leaves, intended to act as a reinforcing phase within the PLA matrix. To enhance the uniform distribution of cellulose in the PLA matrix, ethylene glycol dimethylacrylate (EGDMA) was added as a plasticizer to reduce cellulose aggregation. Moreover, EGDMA acts as a crosslinking agent, promoting the formation of an interconnected polymer network, which enhances structural integrity and dispersion of cellulose within the matrix[14,15]. The nanocomposites were prepared by solution casting technique using different weight percentage of CNFs. The effect of CNFs content (1 and 2wt%) on the pure PLA was evaluated in terms of crystallinity, thermal and antibacterial behaviour of nanocomposites.

MATERIALS AND METHODS

Materials

Matured leaves of screw pine plant were collected from the local areas of kanniyakummari district, Tamil Nadu, India. PLA in the form of granules used as polymer matrix was purchased from 2M biotech LLP natural works (India). Dichloromethane and Sodium hydroxide was received from Spectrochem, (Mumbai). Glacial acetic acid and Sodium chlorite was obtained from Molychem (India). Ethylene glycol dimethyl acrylate was received from Sigma Aldrich. All chemicals were purchased as analytical grade and used as received castor oil of poorna brand was purchased from supermarket. Distilled water was used in this study for the synthesis of cellulose nanofibers.

Isolation of the cellulose nanofibers

The process of extracting CNFs from screw pine leaves involves both mechanical and chemical treatments. Initially, the leaves were cut into 10 mm segments and sun-dried for three days to become brittle. The dried leaves were then ground and sieved into a fine powder. This powder was treated with a 4% sodium hydroxide solution and heated to 80°C for one hour to remove hemicellulose and lignin. The resulting mixture was then filtered and rinsed thoroughly with distilled water to remove all traces of alkali, as confirmed by pH paper. Post-mercerization, the cellulose fibers were bleached using a solution of sodium chlorite and glacial acetic acid at 75°C for three hours to achieve white coloration. After several washings, the fibers were oven-dried at 60°C for two hours to reach a stable weight.

Film preparation

The PLA polymeric solution was prepared by dissolving PLA granules in dichloromethane, followed by continuous stirring until the pellets were

fully dissolved EGDMA was used as a crosslinking agent, and 10% castor oil was added as a plasticizer. The mixture was thoroughly stirred to achieve homogeneity.. The resulting solution was promptly poured onto clean glass mould and left to evaporate at room temperature for 24 hours. The films obtained from this process were designated as pure PLA. To synthesize the nanocomposites CNFs at 1wt% and 2wt% were added to the PLA solution. The CNFs were initially dissolved in the EGDMA solution before being mixed with the PLA solution. This mixture was subsequently cast into plates and allowed to Cure at room temperature for one day. The formed films were labelled as PLAF1 (1wt% CNFs) and PLSF2 (2wt% CNFs). After the preparation, the films were carefully peeled and oven-dried at 60°C, then stored for further analysis.

Characterization

FTIR Spectroscopy

FTIR spectra of the films were obtained using a Fourier Transform Infrared (FTIR) Spectrometer (Thermo Fisher) equipped with a universal attenuated total reflectance (UATR) attachment. The spectra were captured within the frequency range of 4,000 cm^{-1} to 600 cm^{-1}, with a spectral resolution of 4 cm^{-1}.

X-ray diffraction analysis

The XRD pattern of the films were studied from Bruker D8 Advance powder X-ray diffractometer with nickel-filtered Cu Kα radiation (λ = 1.5406 Å). The diffraction data were collected over the 2θ range of 10° to 50° at a scan rate of 0.2° per minute.

Scanning electron microscopy

The morphology of the CNFs and the structure of PLA and PLA nanocomposites were analyzed using a scanning electron microscope (SEM). The specimens were affixed to metal stubs with double-sided tape and gold-coated. Images were captured at 15 kV using a JEOL JSM-840 SEM model.

Thermogravimetric analysis

Thermogravimetric analysis was performed to assess the thermal degradation behavior of the nanocomposites. The thermal stability of each specimen was evaluated using a TGA Q500 series thermogravimetric analyzer (TA Instruments). The analysis was carried out with a heating rate of 20°C per minute under a nitrogen atmosphere.

Antibacterial testing

The prepared films were evaluated for their antibacterial activity using the Kirby-Bauer test against *Staphylococcus aureus* and *Escherichia coli*. The bacteria were spread on the surface of an agar plate, and polymer films and nanocomposite films were placed on top of the bacterial lawn. After 24 h of incubation, the zone of inhibition around the films were measured based on the clear zones surrounding the circular film discs.

RESULTS AND DISCUSSION

FTIR profiling

The FTIR spectra for cellulose nanofibers, pure PLA and the PLA nanocomposite films are presented in the accompanying Fig. 1. For CNFs, a prominent broad absorption band observed at approximately 3410 cm^{-1} is corresponds to the stretching vibrations of free hydroxyl groups. The C–O–C asymmetric stretching and the C–OH stretching vibrations of the glucose rings in cellulose are detected at 1150 cm^{-1} and 1078 cm^{-1} respectively[16]. In case of pure PLA, the absorption bands at 2918 cm^{-1} and 2849 cm^{-1} correspond to the asymmetric and symmetric stretching motions of CH groups within the PLA chains. The absorption band observed at 1650 cm^{-1} is closely associated with the existence of the C=O carbonyl group. Meanwhile, the peak located at 1115 cm^{-1} is linked to the stretching vibrations of the COO group, which signifies the presence of ester linkage. Moreover, the peaks at 874 cm^{-1} and 750 cm^{-1} are associated with the amorphous and crystalline regions of PLA, respectively. A characteristic peak observed at 1254 cm^{-1} found in films containing CNFs, reflects the CO stretching vibrations of cellulose along with residual lignin and hemicellulose. The intensity of the absorption peak at 1647 cm^{-1} shifts to a higher wavenumber due to the disruption of inter- and intramolecular hydrogen bonding in the CNFs, and the intermolecular interactions established between the C=O of PLA and the -OH groups of cellulose nanofibrils. Finally, the displacement of the band within the range of 3321 cm^{-1} to 3418 cm^{-1}

indicates the interactions occurring between PLA and CNF in the nanocomposite. These interactions are primarily attributed to hydrogen bonds formation between the hydroxyl groups present in CNF and the hydroxyl or ester groups in PLA. Such molecular level interactions are crucial, as they can profoundly influence the mechanical and thermal characteristics of the nanocomposite material[17].

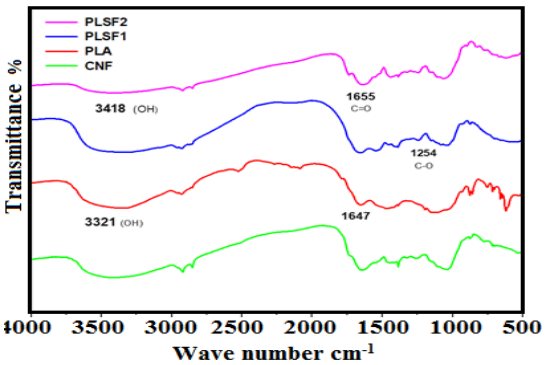

Fig. 1. FTIR spectra of CNF, pure PLA and PLA nanocomposites

Crystallinity behaviour

The XRD patterns of CNF, pure PLA, and the PLA nanocomposite films are displayed in Fig. 2. The CNFs exhibit prominent peak at 22.5°, indicating crystalline regions within cellulose, along with a broader peak around 15.4° that suggests amorphous regions. The particle size of the CNFs, approximately 65 nm as determined from XRD patterns, offer large surface area that improves better dispersion and bonding within the PLA matrix, resulting in a more rigid than pure PLA. The crystallinity index (CrI) was calculated based on the intensity ratio of crystalline to amorphous peaks, revealing the (CrI) of CNFs is 60.5%, reflects their ordered structure, contributing to key properties such as elasticity, thermal stability, and moisture resistance, which improve the composite's mechanical performance[18]. The diffractogram of pure PLA and PLA nanocomposite films, as shown in Fig. 2 indicate a semi-crystalline form. This is evidenced by the presence of a sharp crystalline peak at 16.4° and a broad amorphous peak at 22.5° in both diffraction patterns. The slight shift in diffraction peaks from 16.4° in pure PLA to 16.8° in the PLA nanocomposites indicates an increase in crystallinity, suggesting that CNFs act as nucleating agents. This behavior enhances the formation of crystalline regions within the PLA matrix, promoting the orderly arrangement of PLA chains. As a result, the increased crystallinity likely contributes to improved mechanical strength and thermal stability of the nanocomposite[19].

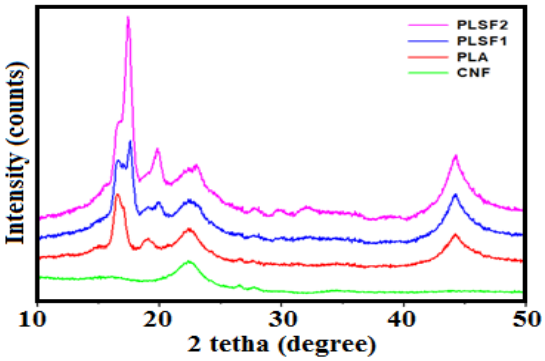

Fig. 2. XRD pattern of CNF, pure PLA and PLA nanocomposites

Morphological studies

SEM analysis is performed to examine the surface morphology of PLA nanocomposites that are reinforced with CNFs. Fig. 3(a) to (d) presents the surface morphology of CNFs, pure PLA and the corresponding nanocomposites. The SEM image of CNFs displays fibrillated morphology with clean and more uniform surface. It is observed that the arrangement of certain fibers in the polymer matrix is in bundled forms, which can be attributed to hydrogen bonding interactions, molecular attraction forces, or mechanical alignment during the preparation phase. As reported by Li *et al.,* chemical purification of cellulose can lead to the formation of large fiber bundles due to strong hydrogen bonding between adjacent CNFs. This bundling effect is consistent with the morphology observed in this study[20]. This alignment is advantageous for nanocomposite materials, improving properties such as tensile strength and load transfer, which leads to a stronger and more effective distribution of stress[17]. The pure PLA shows uniform morphology. Fig. 3(c) and (d) show the inclusion of CNFs created rougher surface with visible pores due to the CNFs dispersion and covered by the PLA matrix. This fine interfacial adhesion between the nanofibres and the polymer matrix would result in an improvement properties of the nanocomposites compared to pure PLA[21].

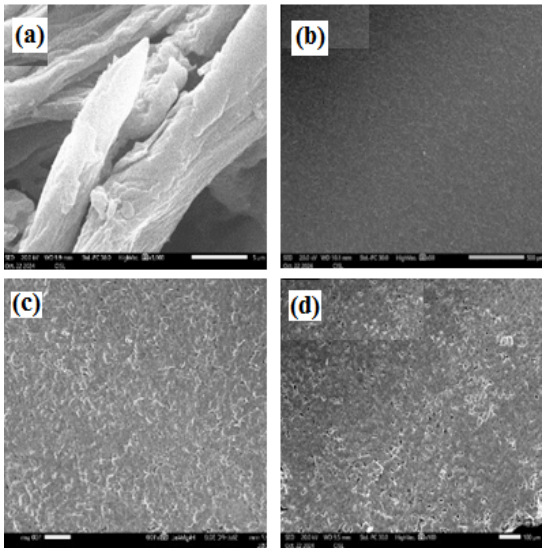

Fig. 3. Surface morphology of (a) CNFs (b) PLA (c) PLPF1 (d) PLSF2

Thermal properties

Thermogravimetric analysis (TGA) was performed to evaluate the thermal stability of the nanocomposites. The weight loss observed in the samples, along with the TGA and DTA curves, is presented in Fig. 4 and Table 1. Fig. 4 illustrates the TGA curves for PLA and PLA nanocomposite, highlighting two distinct regions of weight loss. The initial region, spanning from 75 to 160°C, is associated with moisture loss. The second region, occurring between 285°C and 374°C, corresponds to the structural disintegration of all samples. Above 390°C, involves the breakdown of smaller degradation products, leading to additional weight loss and formation of residues[22]. It has been observed that PLA begins to degrade at roughly 150°C. The weight loss curve for pure PLA reveals 2.5% loss in initial weight up to 285°C, primarily from moisture loss. The degradation process intensifies from 308°C to 343°C, resulting in a weight loss of 50%. This significant reduction is caused by the breaking of ester linkages in the polymer backbones, which produces lactide and other low-molecular weight materials. The main weight loss for PLA nanocomposites, due to CNF and PLA depolymerization, occurs between 282°C and 349°C. Adding 1 and 2wt% CNFs in the PLA matrix reduces the weight loss from 94.3% to 91.2%, indicating improved thermal properties and greater resistance to degradation. It is also noted that the dispersed CNFs contribute to higher degradation temperatures by restricting polymer chain mobility, thus enhancing the nanocomposite's stability. Deng et al. reported that the thermal stability decreases when adding CNFs due to poor dispersion of CNFs[23]. The DTA curves of PLA nanocomposites shift to higher decomposition temperatures with the addition of CNFs. The temperatures are 351°C for PLSF1 and 354°C for PLSF2, compared to 357°C for pure PLA. This indicates that CNFs enhance the thermal endurance of PLA by delaying its degradation[17,24].

Table 1: TGA data of PLA and PLA nanocomposites

Sample	T_{onset} (°C)	$T_{50\%}$ (°C)	T_{max}(°C)	Residue (%)
PLA	146.94	343.92	351.94	1.676
PLSF1	150.02	345.68	354.84	1.738
PLSF2	154.25	349.47	357.99	1.896

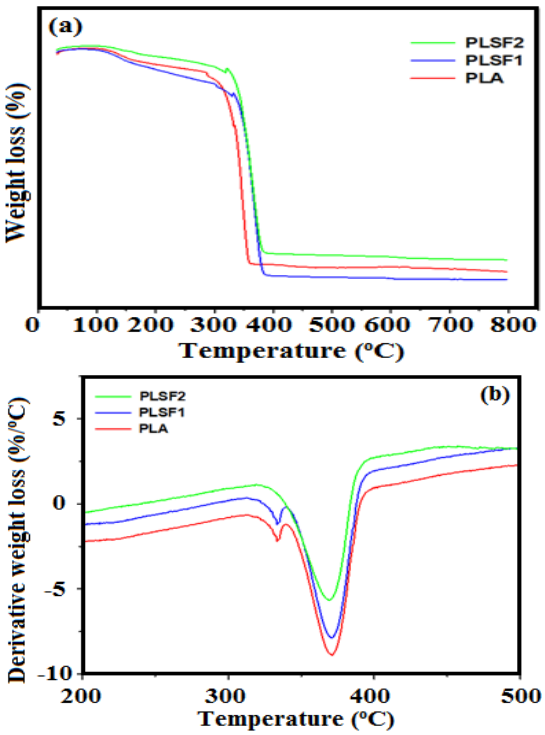

Fig. 4(a). TGA and (b) DTA curves for PLA and PLA nanocomposites

Antibacterial testing

The prepared films were screened for antibacterial activity on the *Gram-positive* bacterium *Staphylococcus aureus* and the *Gram-negative* bacterium *Escherichia coli*. The Fig. 5 and 6 present photographic and bar chart representations of the antibacterial effect of PLA nanocomposite films with 1 and 2wt% CNFs. The PLA nanocomposite film with 2 wt% CNFs (PLSF2) exhibits the highest antibacterial effect, showing a 16 mm reduction in growth for *Staphylococcus aureus* and 16.5 mm for

Escherichia coli. In contrast, the pure PLA film shows the lowest antibacterial activity with zone of inhibition of 14.8 mm for *Staphylococcus aureus* and 14.3 mm for *Escherichia coli*. When compared to the control antibiotic amikacin, which has inhibition zones of 15 mm for *Staphylococcus aureus* and 17 mm for *Escherichia coli*, the PLA nanocomposite films with CNFs demonstrate comparable or slightly lower antibacterial effectiveness against *Escherichia coli* but surpass it in the case of *Staphylococcus aureus*. These observations indicates that the antibacterial effectiveness of the PLA nanocomposite is improved with higher CNFs content. This phenomenon is attributed to the electrostatic interactions that allow CNFs to adhere to bacterial surfaces, leading to the disruption of bacterial cell walls and the inhibition of bacterial growth[25].

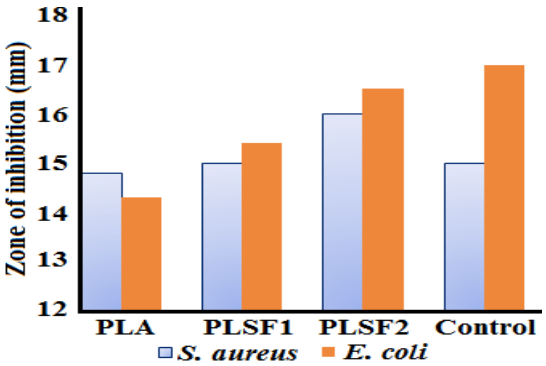

Fig. 5. Antibacterial activity of PLA and PLA nanocomposites

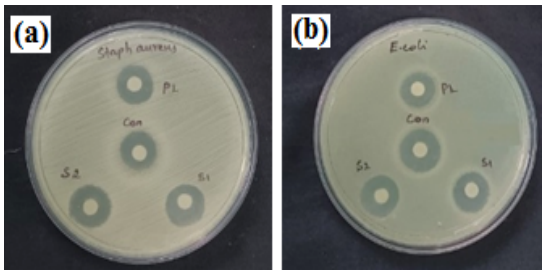

Fig. 6. Antibacterial behaviour of (a) *S. aureus* (b) *E. coli*

CONCLUSION

Incorporating CNFs provides a sustainable approach to enhancing the properties of PLA without compromising its biodegradable nature. FTIR analysis confirms that the interaction between the carbonyl of PLA and the hydroxyl (OH) of CNFs improves compatibility and dispersion within the PLA matrix. XRD studies show that CNFs have crystallinity index of 60.5%, which contributes to the mechanical reinforcement of the nanocomposite. Moreover, the increased crystallinity of the PLA nanocomposite compared to pure PLA, indicating enhanced structural properties. Thermal analysis shows that the PLA nanocomposites can tolerate temperature upto 300°C. The SEM analysis further confirms that CNF isolation achieves nanoscale fibrillation, increasing surface area and promoting better integration within the PLA matrix. Antibacterial testing demonstrates that the PLA nanocomposites possess good antibacterial activity against common pathogens, making them suitable for applications requiring antibacterial efficiency. Overall, these improvements position PLA nanocomposite films as promising candidates for sustainable packaging, biomedical, and hygiene applications, combining enhanced crystallinity, thermal stability, and antibacterial properties with environmental compatibility.

ACKNOWLEDGEMENT

The authors express their gratitude to VOC College, Tuticorin, VIT Institute of Technology, Vellore, Annamalai University, Chennai, and Manonmaniam Sundaranar University, Tirunelveli, Scudder Medical Laboratory, Nagercoil for their support in sample testing.

Conflict of interest

The authors stated that there is no conflict of interests related to the publication of this article.

REFERENCES

1. Drumright, R. E.; Gruber, P. R.; Henton, D. E., *Polylactic Acid Technology. Adv. Mater.*, **2000**, *12*(23), 1841-1846.
2. Auras, R.; Harte, B.; Selke, S. An Overview of Polylactides as Packaging Materials., *Macromol. Biosci.*, **2004**, *4*(9), 835-864.
3. Lunt, J. Large-scale production, properties and commercial applications of polylactic acid polymers., *Polym. Degrad. Stab.*, **1998**, *59*(1-3), 145-152.
4. Gupta, A. P.; Kumar, V. New emerging trends in synthetic biodegradable polymers – Polylactide: A critique., *Eur. Polym. J.*, **2007**, *43*(10), 4053-4074.
5. Moon, R. J.; Martini, A.; Nairn, J.; Simonsen, J.; Youngblood, J. Cellulose nanomaterials review: structure, properties and nanocomposites., *Chem. Soc. Rev.*, **2011**, *40*(7), 3941-3994.

6. Eichhorn, S. J.; Dufresne, A.; Aranguren, M. Review: current international research into cellulose nanofibres and nanocomposites., *J. Mater. Sci.*, **2010**, *45*(1), 1-33.
7. Zhou, Y. M.; Fu, S. Y.; Zheng, L. M.; Zhan, H. Y. Effect of Nanocellulose Isolation Techniques on the Formation of Reinforced Poly (Vinyl Alcohol) Nanocomposite Films., *Express Polym. Lett.,* **2012**, *6*, 794-804.
8. Tappanawatch, W.; Prapainainar, P.; Sae-Oui, P.; Loykulnant, S.; Dittanet, P. Effect of Gamma Radiation on Properties of Cellulose Nanocrystal/Natural Rubber Nanocomposites., *Key Eng. Mater.*, **2018**, *772*, 13-17.
9. Tang, J.; Sisler, J.; Grishkewich, N.; Tam, K. C. Functionalization of cellulose nanocrystals for advanced applications., *J. Colloid Interface Sci.*, **2017**, *494*, 397-409.
10. Adkar, P. P.; Bhaskar, V. H. Pandanus odoratissimus (Kewda): A Review on Ethnopharmacology, Phytochemistry, and Nutritional Aspects., *Adv. Pharmacol. Sci.*, **2014**, Article ID 120895.
11. Raina, V. K.; Kumar, A.; Srivastava, S. K.; Syamsundar, K. V.; Kahol, A. P. Essential oil composition of 'kewda' (Pandanus odoratissimus) from India., *Flavour Fragr. J.*, **2004**, *19*(5), 434-436.
12. Noremylia, M. B.; Hassan, M. Z.; Ismail, Z. Recent advancement in isolation, processing, characterization and applications of emerging nanocellulose: A review. *Int. J. Biol. Macromol.,* **2022**, *206*, 954-976.
13. Miao, X.; Lin, J.; Tian, F.; Li, X.; Bian, F.; Wang, J. Cellulose nanofibrils extracted from the byproduct of cotton plant., *Carbohydr. Polym.*, **2016**, *136*, 841-850.
14. Bin, Y.; Yang, B.; Wang, H. The effect of a small amount of modified microfibrillated cellulose and ethylene–glycidyl methacrylate copolymer on the crystallization behaviors and mechanical properties of polylactic acid., *Polym. Bull.*, **2018**, *75*, 3377-3394.
15. Bijarimi, M.; Ahmad, S.; Rasid, R.; Khushairi, M. A.; Zakir, M. Poly(lactic acid) / Poly(ethylene glycol) blends: Mechanical, thermal and morphological properties., *AIP Conference Proceedings* 1727, 020002 (**2016**).
16. Frone, A. N.; Berlioz, S.; Chailan, J. F.; Panaitescu, D. M. "Morphology and thermal properties of PLA–cellulose nanofibers composites,"*Carbohydr. Polym.*, **2013**, *91*, 377-384.
17. Frone, A. N.; Panaitescu, D. M.; Chiulan, I.; Nicolae, C. A.; Vuluga, Z.; Vitelaru, C.; Damian, C. M. The effect of cellulose nanofibers on the crystallinity and nanostructure of poly(lactic acid) composites., *J. Mater. Sci.*, **2016**, *51*(14), 9771-9791.
18. Rao, S.; Madhushree, M.; Bhat, K. S. Characteristics of surface modified sugarcane bagasse cellulose: application of esterification and oxidation reactions., *Sci. Rep.*, **2024**, *14*, 24136.
19. Agbakoba, V. C.; Mokhena, T. C.; Ferg, E. E.; Hlangothi, S. P.; John, M. J. PLA bio-nanocomposites reinforced with cellulose nanofibrils (CNFs) for 3D printing applications., *Cellulose.*, **2023**, *30*, 11537-11559.
20. Poletto, M.; Pistor, V.; Zattera, A. J. Structural characteristics and thermal properties of native cellulose., *Cellulose.*, **2013**, *20*(1), 2081-2091.
21. Li, J.; Li, J.; Feng, D.; Zhao, J.; Sun, J.; Li, D. Comparative study on properties of polylactic acid nanocomposites with cellulose and chitin nanofibers extracted from different raw materials., *J. Nanomater.,* **2017**, *3*, 1.
22. Wang, Q.; Ji, C.; Sun, J.; Zhu, Q.; Liu, J. Structure and properties of polylactic acid biocomposite films reinforced with cellulose nanofibrils., *Molecules.*, **2020**, *25*(14), 3306.
23. Ruz-Cruz, M. A.; Herrera-Franco, P. J.; Flores-Johnson, E. A.; Moreno-Chulim, M. V.; Galera-Manzano, L. M.; Valadez-Gonzalez, A. Thermal and mechanical properties of PLA-based multiscale cellulosic biocomposites., *J. Mater. Res. Technol.*, **2022**, *18*, 485-495.
24. Deng, Z.; Wu, Z.; Tan, X.; Deng, F.; Chen, Y.; Chen, Y.; Zhang, H. Preparation, Characterization, and Antibacterial Property Analysis of Cellulose Nanocrystals (CNC) and Chitosan Nanoparticles Fine-Tuned Starch Film., *Molecules.*, **2022**, *27*, 8542.
25. Duygulu, N. E.; Ciftci, F.; Ustundag, C. B. Electrospun drug blended poly(lactic acid) (PLA) nanofibers and their antimicrobial activities., *J. Polym. Res.*, **2020**, *27*, 232.